Understanding Calendar Aging of Thiophosphate-Based Solid-State Batteries

Journal of The Electrochemical Society, 2025 **172** 100519
1945-7111/2025/172(10)/100519/13/$40.00 © 2025 The Electrochemical Society ("ECS"). Published on behalf of ECS by IOP Publishing Limited.

Understanding Calendar Aging of Thiophosphate-Based Solid-State Batteries

Ruihao Deng, Ratnottam Das, Ruixin Wu, Keng Xu, Bowen Shao, and Fudong Han[z]

Department of Mechanical, Aerospace and Nuclear Engineering, Rensselaer Polytechnic Institute, Troy, New York 12180, United States of America

While significant progress has been made to improve the energy density, power density, and cycle life of solid-state batteries (SSBs), their calendar life, which dictates the capacity retention during storage, has been seldom studied. One key difference between liquid electrolytes and solid electrolytes is the residual electronic conductivity in solids. Despite being small, the electronic conductivity in solid electrolytes can lead to perceptible self-discharge especially when the battery is not under constant use. However, its contribution to the calendar decay of SSBs has not been considered with existing studies solely focusing on the irreversible capacity loss caused by the side reactions between electrodes and solid electrolytes. Here, we present our study on calendar aging of Li_6PS_5Cl-based SSBs throughout 8 months of measurement at 25 and 60 °C. We report that apparent capacity decay, 4.1% at 25 °C and 7.0% at 60 °C, occurs over the entire period of the test, highlighting the critical challenge of calendar aging of SSBs. More importantly, by quantifying the irreversible and reversible capacity losses, we demonstrate the predominant role of reversible self-discharge during calendar aging of SSBs and provide new insights into improving the calendar life of SSBs.
 [DOI: 10.1149/1945-7111/ae0f59]

Manuscript submitted August 8, 2025; revised manuscript received September 25, 2025. Published October 14, 2025.

Although lithium-ion batteries (LIBs) have enjoyed unprecedented growth and success in powering portable electronics and small electric tools, they face challenges in safety, energy density, service life, and cost for the applications of electrifying transportation and grid storage.[1] Solid-state batteries (SSBs) based on thiophosphate solid electrolytes such as Li_6PS_5Cl, $Li_{10}GeP_2S_{12}$, and Li_2S-P_2S_5, are considered a very promising candidate for next-generation energy storage due to their great potential to improve safety, energy density, fast charging capability, and cycle life compared with today's LIBs based on liquid electrolytes.[2–6] While a longer cycle life is certainly necessary, it is not the only metric that determines the service life of a battery because the capacity loss can be caused by both cycling aging, i.e., capacity decay during repeated charge/discharge cycles, and calendar aging, i.e., capacity decay during storage.[7–10] In real-world scenarios, calendar aging can play a much bigger role than cycling aging because the operation periods are substantially shorter than the idle intervals. For example, electric vehicles (EVs) are idle for more than 90% of the time.[11–13] Although calendar aging and cycling aging share many similar mechanisms, a long cycle life does not necessarily indicate a long calendar life, as demonstrated in Si-containing anodes.[14–16] Current liquid-electrolyte Li-ion batteries based on graphite-based anodes have been reportedly demonstrated to have a long calendar life of >15 years.[17] Understanding the mechanism of calendar aging of thiophosphate-based SSBs is critical to determine whether they can exhibit a comparable or better calendar life but has rarely been studied.

The calendar aging of conventional liquid-electrolyte-based LIBs is known to be a result of several simultaneous physicochemical processes: loss of lithium inventory (LLI), loss of active material (LAM), impedance rise, and reversible self-discharge (Fig. 1).[8,10,18] A typical example for LLI is the growth of solid electrolyte interphase (SEI) where the electrolyte reduction leads to lithium incorporation into the SEI and this lithium is no longer available between the electrodes.[10] lAM can be caused by electrode dissolution, irreversible side reactions with the electrolytes, irreversible phase transition (e.g., from layered to rock-salt) or local structural evolution (e.g., Li/Ni site switching), electrode particle isolation, and electrode delamination during calendar aging.[19] Impedance rise in the cell can also occur during calendar aging, for example, by excessive electrolyte consumption (also referred to as electrolyte dry-out), leading to a decrease of the deliverable capacity of the cell under a fixed voltage range for charge/discharge. All the above-mentioned three aging mechanisms can be considered as irreversible capacity loss, i.e., the capacity decreased during aging cannot be recovered upon subsequent charging. However, reversible self-discharge can also occur in liquid-electrolyte LIBs during calendar aging due to coupled side reactions between the cathode and the anode.[18,20] One example is through the CO_2 shuttle mechanism. CO_2 in the electrolyte will be reduced at the anode, forming oxalate ($C_2O_4^{2-}$) that can diffuse back to the cathode and be oxidized back to CO_2, leading to a net result of two Li ions transferring from the cathode to the anode internally.[21,22] Amongst all the above processes, LLI caused by SEI growth has been demonstrated as the dominant mechanism in liquid-electrolyte-based LIBs.[8] A recent study that analyzed the capacity loss of various cell chemistries from existing literature results also suggests a strong $t^{1/2}$ dependency.[8] The exact calendar life strongly depends on the quality of the SEI, which is also the reason why graphite has a better calendar life than Si-based anodes.[15]

While all the physicochemical processes, including LLI, LAM, impedance rise, and reversible self-discharge, could also occur in SSBs, due to the different properties between solid electrolytes and liquid electrolytes, there can be distinct differences in the causes and relative contribution of each process to the overall calendaring decay (Figs. 1a and 1b). Firstly, most liquid electrolytes exhibit better stability at high voltages than at low voltages, leading to a much more pronounced formation of SEI than CEI in typical LIBs. However, many solid electrolytes exhibit limited electrochemical stability at both high voltages and low voltages.[23–25] As a result, side reactions with the solid electrolyte will occur at both the cathode and the anode.[26,27] The side reaction between solid electrolytes and cathodes can not only lead to the apparent growth of cathode electrolyte interphase (CEI), which enhances LLI, but also promote loss of cathode active material (LAM) due to irreversible side reactions between the solid electrolyte and the cathode.[27,28] Secondly, solid electrolytes are not flowable and infiltrative as liquids. Although the non-infiltrative feature of solid electrolytes helps to form a less dynamic SEI/CEI (i.e., no need to reform part of the SEI/CEI upon cracking or pulverization),[29,30] which will help mitigate LLI, it will lead to a more severe issue in LAM because of the challenge to keep the interfacial contact between solid electrolytes and electrodes due to side-reaction-induced contact loss (so-called "chemo-mechanical degradation"),[28] electrode cracking and pulverization during calendar aging. The third difference in SSBs is the absence of electrode dissolution in electrolytes. This not only eliminates LAM caused by electrode dissolution but also prevents reversible self-discharge due to coupled side reactions between the

[z]E-mail: hanf2@rpi.edu

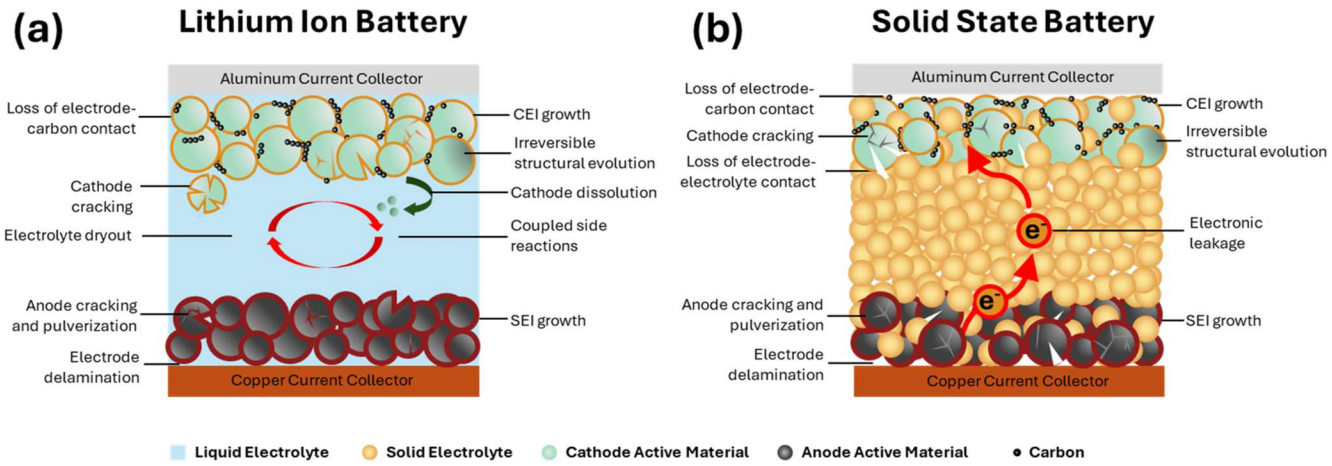

Figure 1. Calendar aging mechanisms in liquid-electrolyte lithium-ion batteries and solid-state batteries.

cathode and the anode. Another distinct difference between solid and liquid electrolytes is the existence of residual electronic conductivity in solids. Although the electronic conductivity is typically orders of magnitude lower than the ionic one in solid electrolytes, it is never zero and therefore can lead to perceptible reversible self-discharge especially when the battery is not under constant use.[31,32]

Because of these differences, the capacity decay during calendar aging of thiophosphate-based SSBs may be governed by different mechanisms from the conventional wisdom learned from LIBs. While the electrochemical stability of thiophosphate-based solid electrolytes is limited at both high and low voltages, the SEI formed at the interface between solid electrolytes (e.g., Li_6PS_5Cl and Li_3PS_4) and Li metal anodes is quite passivating.[33–35] The growth of the SEI layer at the Li/SE interface is very limited during long-term storage.[36] This is also probably the reason why the only few studies on calendar aging of SSBs all focused on LLI and LAM caused by the side reactions between layered oxide cathodes and solid electrolytes.[25,37–41] Ceder et al. highlighted the importance of interfacial instability, especially at high temperature and high state-of-charge (SOC), on the calendar life of SSBs.[25] Kang et al. reported the first experimental study on the detrimental effect of high-temperature storage of Li_6PS_5Cl-based SSBs due to the electrolyte decomposition at the interface with $LiNi_{0.8}Mn_{0.1}Co_{0.1}O_2$ cathode.[39] Through a series of careful structural characterizations, Yoon et al. confirmed the enhanced side reactions between Ni-rich cathodes and the lithium argyrodite-type solid electrolyte during high-temperature storage.[37] A recent study from Yang et al. also reported that the $LiNi_{0.8}Mn_{0.1}Co_{0.1}O_2$ cathode composite with Li_6PS_5Cl solid electrolyte exhibits a much better capacity retention during aging than the cathode with a bi-electrolyte (Li_3YCl_6-Li_6PS_5Cl) due to the differences in the cathode/electrolyte reactions.[39] By comparing the stability of cathode/electrolyte and anode/electrolyte interfaces, Lee et al. first demonstrated that the calendar aging of the anode-free SSB with a $LiNi_{0.88}Co_{0.09}Al_{0.03}O_2$ cathode, Li_6PS_5Cl solid electrolyte and an Ag-C anode interlayer, is dominated by the side reactions between the cathode and the solid electrolyte, rather than the anode/electrolyte interface.[40] Most recently, Wu et al. demonstrated that $LiCoO_2$-Li_6PS_5Cl cathode experiences much less capacity decay compared with $LiNi_{0.8}Co_{0.1}Mn_{0.1}O_2$-$Li_6PS_5Cl$ cathode during calendar aging due to the different extent of side reactions at a high temperature and a high SOC.[41]

While LLI and LAM caused by side reactions between the cathode and the solid electrolyte will certainly be involved in SSBs, leading to irreversible capacity losses, none of the previous studies investigated the effect of residual electronic conductivity of solid electrolyte on reversible capacity loss during calendar aging. While reversible self-discharge seems to be not as detrimental as irreversible ones, it is critical for applications that do not need frequent charging such as backup power, seasonal equipment, or primary energy-storage systems, and more importantly, it can lead to perceptible energy loss regardless of the application. A recent study from Shao et al. suggests that the electronic conductivity of many excellent solid electrolytes including thiophosphates ($\sim 10^{-10}$ S cm^{-1}) is orders of magnitude higher than that of LiPON (10^{-14} and 10^{-13} S cm^{-1}), and the long calendar life of LiPON-based thin-film batteries[42] cannot be assumed for bulk-type solid-state batteries based on thiophosphate electrolytes.[31] In fact, apparent reversible self-discharge due to electronic leakage was also observed in Wu et al.'s work by monitoring the open circuit voltage of the cell during high-temperature aging.[41] In this work, we aim to understand the mechanisms of calendar aging of thiophosphate-based SSBs by measuring their capacity decay throughout 8 months of aging at 25 and 60 °C. Different from the previous studies that solely focus on irreversible calendar decay caused by side reactions between the cathode and the solid electrolyte, we also quantify the reversible capacity loss to understand the relative contribution of irreversible and reversible decay mechanisms to the overall calendar decay. The results suggest the important role of electronic leakage in the calendar decay of solid-state batteries and point to new directions for further improving the calendar life of thiophosphate-based SSBs.

Results and Discussion

The calendar aging measurement was performed with a typical cell structure used in the solid-state battery community (Fig. 2a).[6] The cathode consisted of $LiNbO_3$-coated $LiCoO_2$ and Li_6PS_5Cl with a weight ratio of 70:30. li_6PS_5Cl was used as a solid electrolyte and the thickness of the electrolyte is around 800 μm. $Li_{0.5}In$ was used as the anode due to its excellent stability with Li_6PS_5Cl. Since electronic leakage strongly depends on the electronic conductivity of solid electrolyte, we used Li_6PS_5Cl synthesized in house to ensure consistency of the measurement. Figures A·1–A·3 compare the Li_6PS_5Cl synthesized in-house with the samples from the commercial suppliers, and the results suggest that the Li_6PS_5Cl used in this study is of high quality with high purity, a superior ionic conductivity (4.3 mS cm^{-1}) and low electronic conductivity (3.4×10^{-10} S cm^{-1}) at room temperature. The test protocol for calendaring aging consists of five formation cycles followed by seven aging/diagnostic blocks. The aging was performed at 100% SOC and the duration for the aging period is 1 month except for the second aging which is 2 months, leading to the total aging time of 8 months (Fig. 2b). Each diagnostic process includes 1st discharge to 3.0 V immediately after aging and two complete cycles between 3.0 V to 4.2 V. The cell was then charged by a constant current constant voltage (CCCV) protocol to 4.2 V to ensure the cell was aged at 100% SOC. A typical constant current (CC) charging and discharging protocol was used for the cells without aging as the control cells.

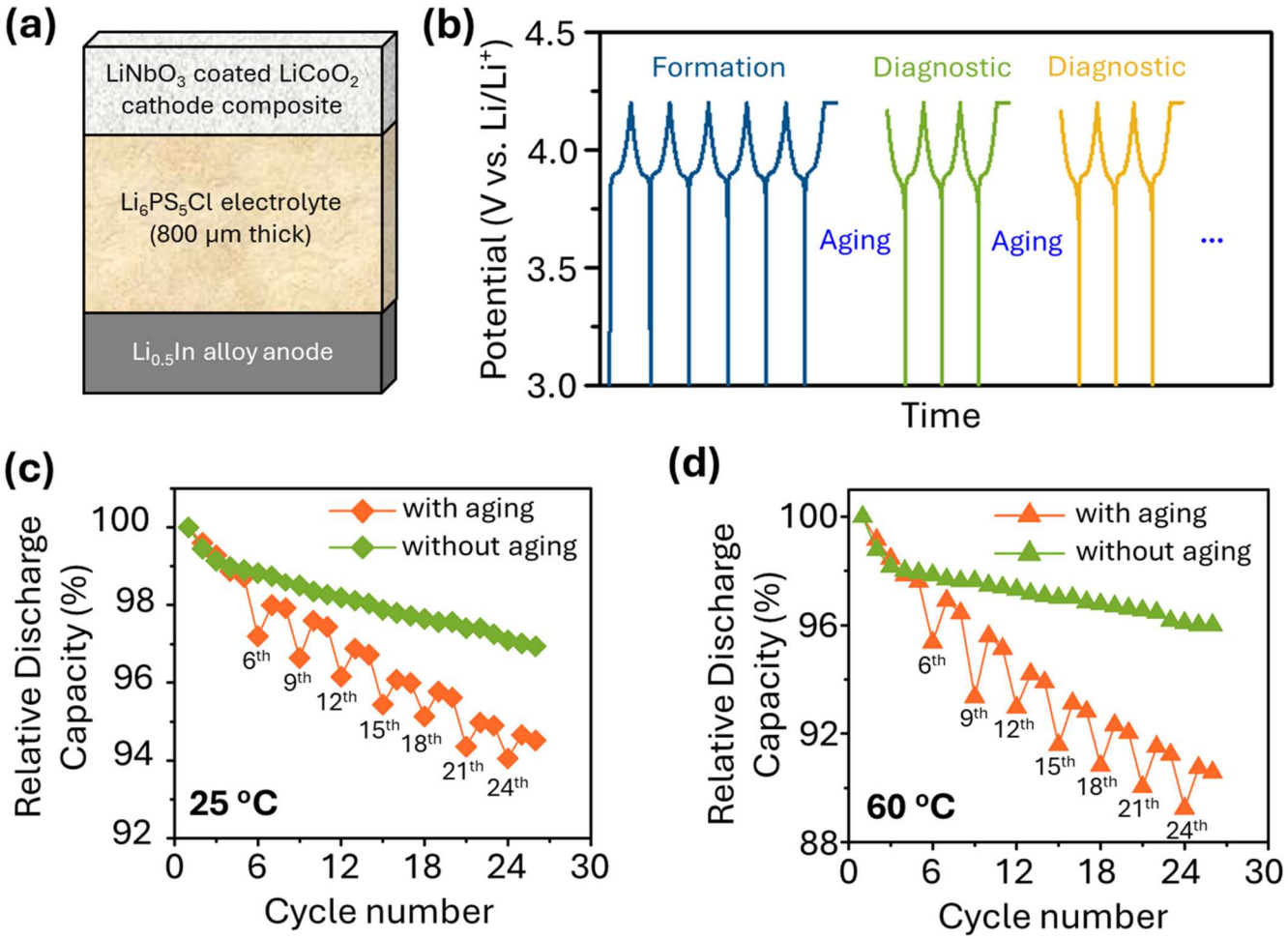

Figure 2. (a) **Cell structure**. The studied SSB consists of a $LiNbO_3$-coated $LiCoO_2$ cathode, an 800 μm-thick Li_6PS_5Cl solid electrolyte, and a Li-In alloy anode. (b) **Test protocol**. After 5 formation cycles at C/20, the cell undergoes a CCCV charging to 4.2 V, followed by seven aging/diagnostic blocks. Each aging/diagnostic block includes an aging period, a discharge process at C/20 directly after aging, two cycles at C/20, followed by a CC charging at C/20 to 4.2 V and a CV charging at 4.2 V for 12 h to equilibrate the cell at 100% SOC. The duration of the aging period is 1 month except for the 2nd aging which is 2 months. (c and d) Discharge capacities at different cycles during testing with and without aging at 25 °C (c) and 60 °C (d). The discharge capacity was normalized based on the discharge capacity from the formation cycles.

Figure 2 shows the evolution of the discharge capacities of the cells at different cycles at 25 °C (Fig. 2c) and 60 °C (Fig. 2d). Since the capacity decay can be caused by both cycling aging and calendar aging during the test, we compared the capacity loss of the cell with and without aging. Although a quick capacity decay can be observed during formation cycles due to the stabilization of the interphases, the cells experienced a much faster capacity decay during the subsequent cycles with aging compared with those without aging at both temperatures, indicative of apparent calendar decay. The capacity loss at a higher temperature is larger than that at a lower temperature. While a gradual decrease of the capacity with cycles can be observed during testing without aging, there are some "valleys" for the discharge capacity right after aging (Figs. 2c and 2d, i.e., the discharge capacity decreases right after aging (cycle 6th, 9th, 12th…) and then increases back for the subsequent diagnostic cycle (cycle 7th, 10th, 13th…). The results suggest that capacity loss can be recovered upon subsequent charge, which is a strong indication of reversible capacity loss. The capacity loss is so large that we cannot see the capacity increase due to CCCV charging (compared with the CC charging) before the aging period. The results clearly suggest that electronic leakage plays a critical role in the capacity decay of SSBs.

To understand the capacity decay during the test, we plotted the discharge capacities right after each aging, denoted as the 1st discharge capacity, and the discharge capacity for the subsequent diagnostic cycle, denoted as the 2nd discharge capacity, with increasing aging durations (Fig. 3a). Both capacities have important implications in the practical application. The 1st discharge capacity indicates the remaining capacity of the cell after experiencing all decay mechanisms including both cycling decay and calendar decay, while the 2nd discharge capacity provides information on the remaining capacity only due to irreversible decay mechanisms. The capacity retentions of 1st and 2nd discharge processes after 8-month storage are 95.9% and 95.3% at 25 °C, and 93.0% and 91.4% at 60 °C, respectively. The gap between the 1st and 2nd discharge capacity is related to the reversible capacity loss. The larger gap observed at a higher temperature is consistent with the increase of electronic conductivity with temperature (Figs. A·3 and A·4).

We then investigated the trend of the decay of the 2nd discharge capacity after different aging periods. Previous research on calendar aging of LIBs suggests that irreversible capacity decay follows a power law relation with time.[8,13] Most studies suggest the capacity decay follows a square root of time relationship because the side reactions between electrodes and electrolytes as well as SEI growth can be considered a diffusion-controlled process.[8] However, no such power law relationship can be observed for SSBs studied in this work. The detailed reason for such behavior is currently unknown but might be related to LAM caused by non-side-reaction-related mechanisms such as irreversible structural degradation of the cathode active material itself. Based on the existing data, we applied

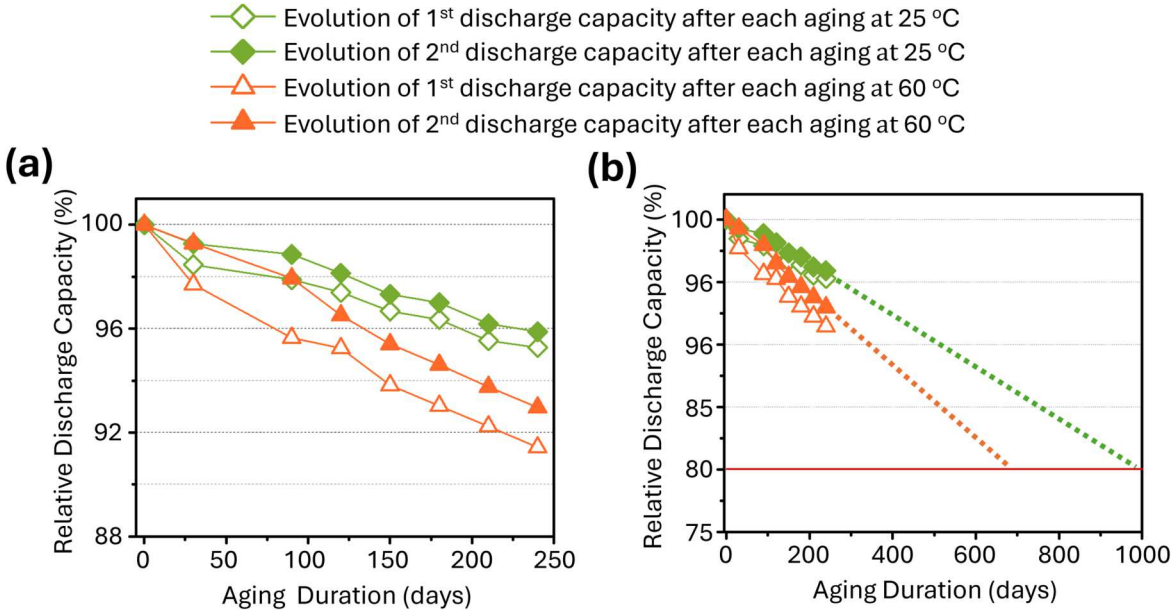

Figure 3. (a) Evolutions of the 1st and 2nd discharge capacities after different aging durations at 25 and 60 °C. (b) Projections of the capacity decay to estimate the calendar life of the studied SSBs at 25 and 60 °C.

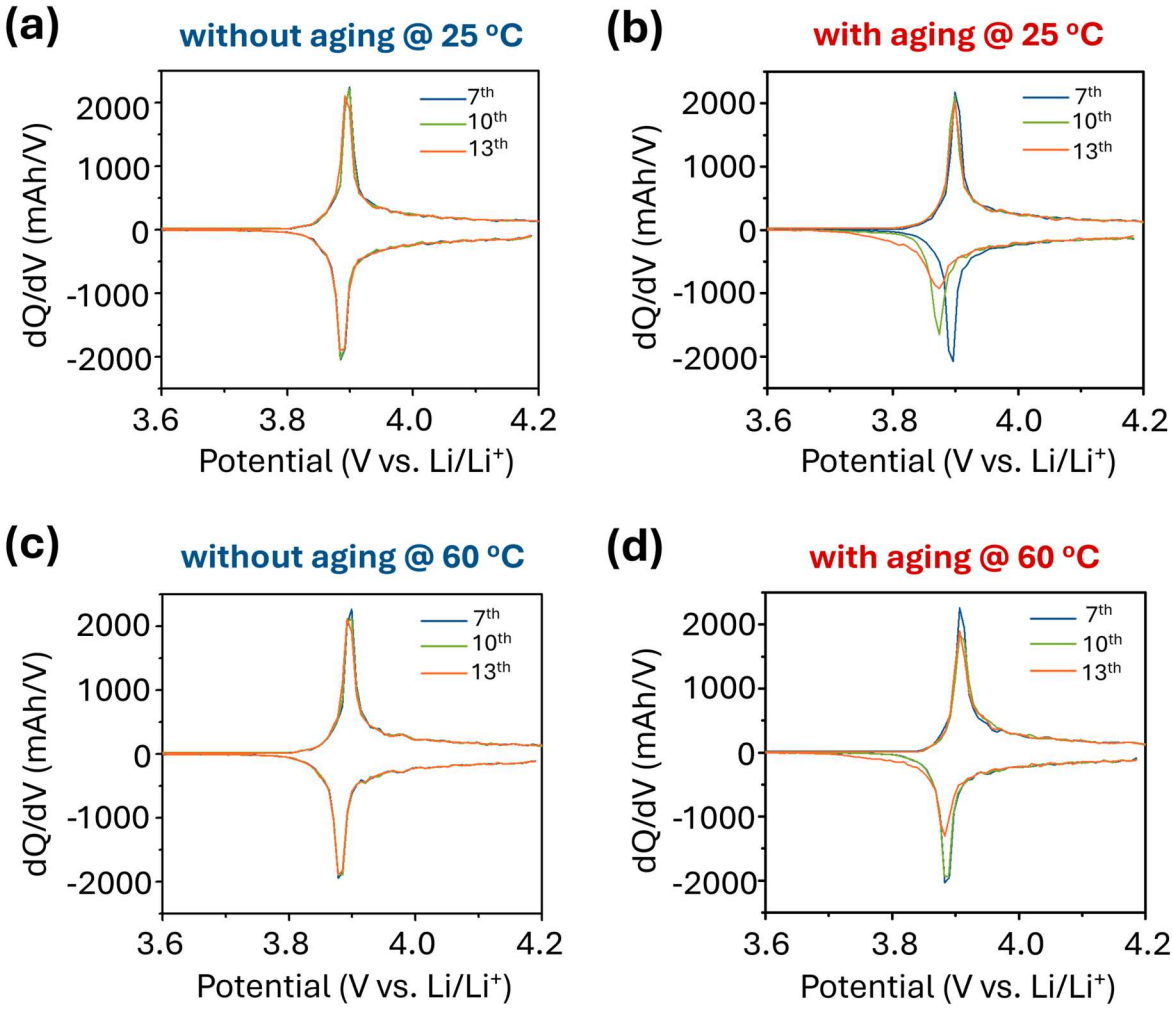

Figure 4. (a) and (b) Differential capacity vs voltage (dQ/dV) curves for testing at 25 °C without aging (a) and with aging (b). (c) and (d) Differential capacity vs voltage (dQ/dV) curves for testing at 60 °C without (c) and with aging (d).

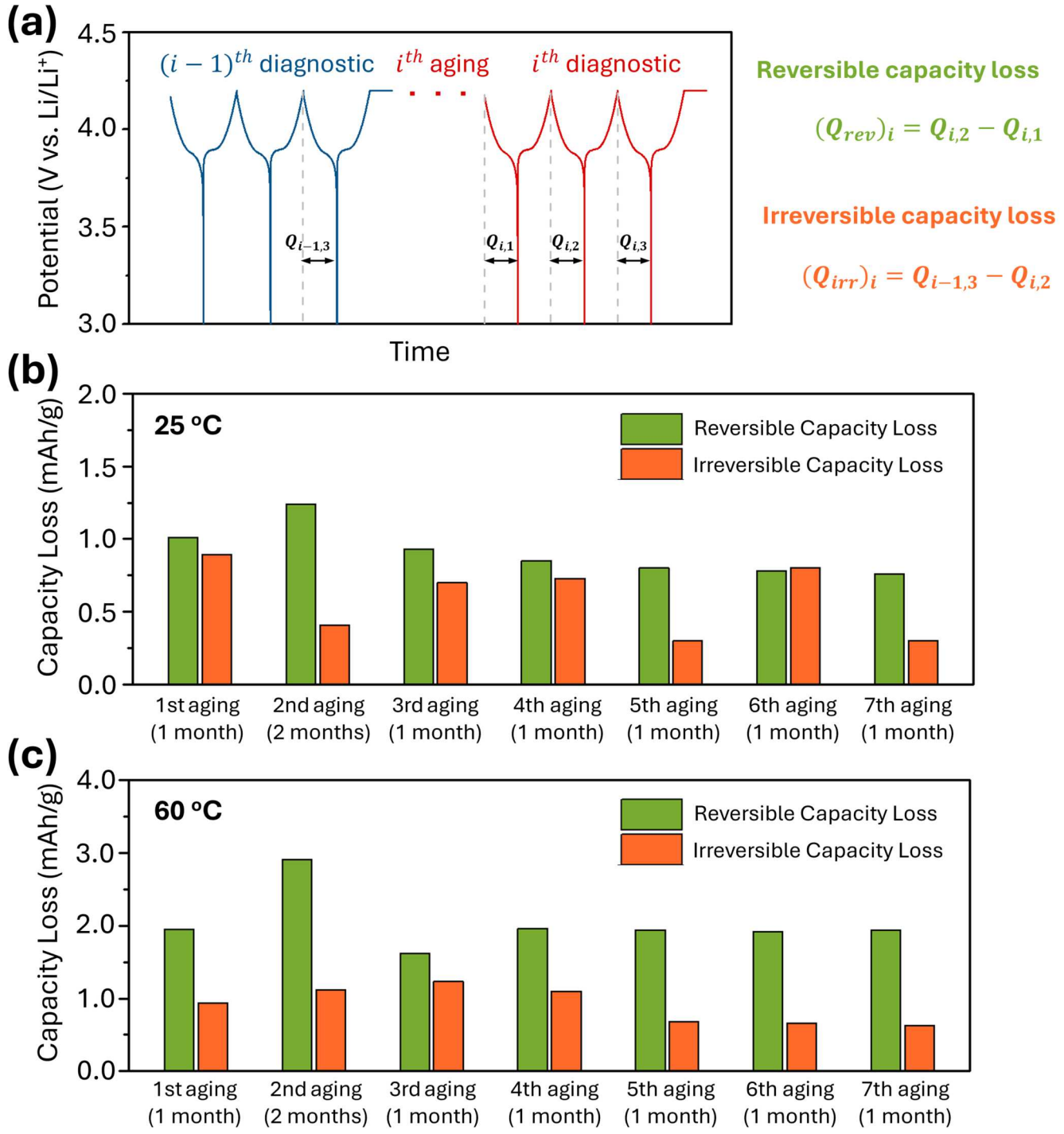

Figure 5. (a) Schematic showing how to determine reversible capacity loss and irreversible capacity loss. (b) and (c) Comparison of reversible and irreversible capacity losses after each aging test at 25 °C (b) and 60 °C (c).

a simple linear extrapolation to estimate the capacity decay over a long period of aging (Fig. 3b). The projection in Fig. 3b shows that the calendar life, where the capacity drops to 80%, is around 1000 days at 25 °C and around 700 days at 60 °C. While the calendar life is certainly dependent on the cell form factor and testing protocol, such a limited calendar life for SSBs with a relatively stable $LiNbO_3$-coated $LiCoO_2$ cathode,[43] an 800 μm-thick solid electrolyte, and a relatively stable Li-In anode is still quite alarming.

It should be noted that the irreversible capacity decay of SSBs in Fig. 3 is caused by both cycling aging and calendar aging, even if the cells experienced only a relatively small number of cycles. Quantifying the individual contribution of calendar aging and cycling aging to the overall capacity decay is challenging, even for industrial standardized cells with well-known chemistry, because of their coupling effects.[44,45] To understand the effect of cycling aging and calendar aging on the degradation of the cathode, we performed differential capacity vs voltage (dQ/dV) analysis for cycles 7th, 10th, and 13th for cells with and without aging (Fig. 4). Because of the excellent stability of the Li-In anode with Li_6PS_5Cl solid electrolyte and the excessive Li inventory in the cell, the dQ/dV curves mainly reflect the charge/discharge behavior of the cathode. The charge/discharge curves used for the analysis are shown in Fig. A·5. No apparent changes in the dQ/dV curves can be observed for the cells tested without aging at both temperatures (Figs. 4a and 4c). For the

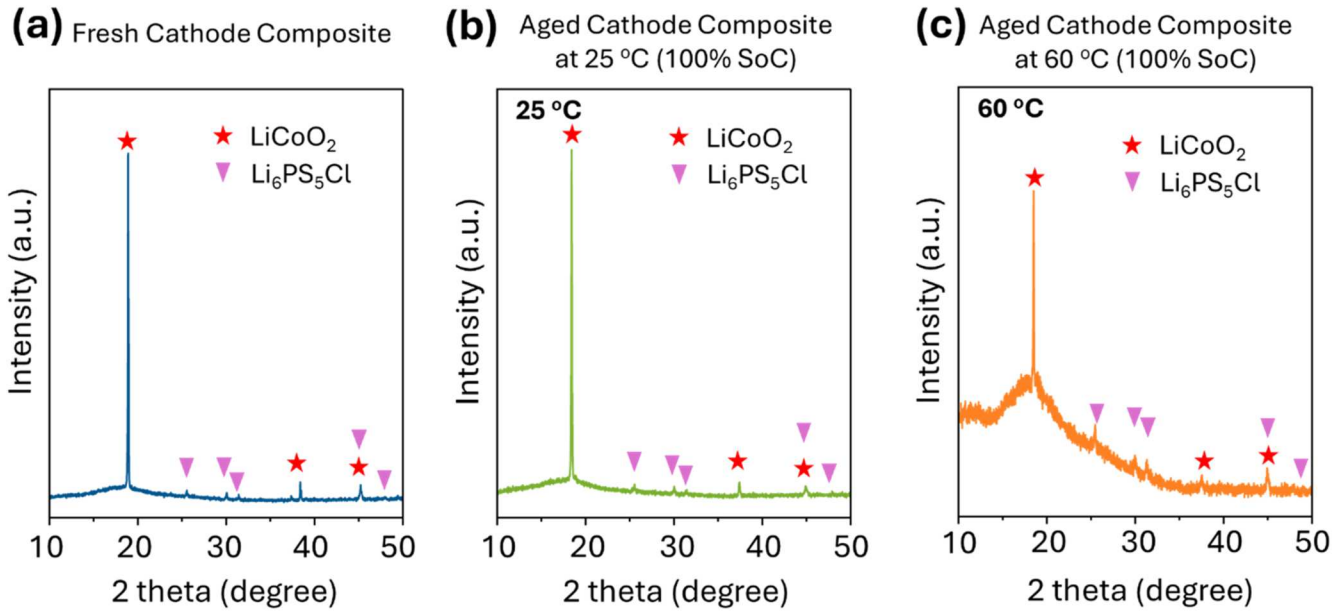

Figure 6. XRD of the $LiCoO_2$-Li_6PS_5Cl cathode composite before (a) and after aging at 100% SOC for 8 months at 25 °C (b) and 60 °C (c).

cells that experienced aging, the peak for the discharging process shifted to a low potential accompanied by a slight decrease in the peak intensity for the charging process (Figs. 4b and 4d), indicative of irreversible degradation of the cathode. The results indicate that calendar aging at 100% SOC plays a more important role in the deterioration of the cathode than cycling aging. It should also be noted that the testing protocol for calendar aging can have a large impact on the results,[46] and for the present study, the constant voltage charging step for 12 h to 100% SOC may lead to irreversible side reactions between the cathode and the solid electrolyte.[39] To understand its effect on the overall calendar decay, we also performed a dQ/dV analysis of SSBs tested with constant voltage charging and without aging (Fig. A·6), and only minimal change can be observed in the dQ/dV curves for the 7th, 10th and 13th cycles. The results suggest that, while irreversible capacity loss due to cycling aging certainly exists, a majority of the irreversible capacity decay is due to calendar aging.

To elucidate the relative contribution of irreversible and reversible capacity loss during calendar aging, we extracted the irreversible and reversible capacity losses after each aging (Fig. 5). As demonstrated in Fig. 5a, the reversible capacity loss is determined by subtracting 1st discharge capacity from the 2nd discharge capacity within each diagnostic block, and the irreversible capacity loss is determined by subtracting the 2nd discharge capacity of the current diagnostic block from the 3rd discharge capacity of the previous diagnostic cycle. Figures 5b and 5c compare the irreversible capacity loss and reversible capacity loss at 25 and 60 °C. Except for the 6th aging at 25 °C, the reversible capacity losses are larger than the irreversible ones at both 25 °C (Fig. 5b) and 60 °C (Fig. 5c), suggesting the critical role of electronic leakage in the capacity decay during aging. The electronic leakage-induced capacity decay is also supported by the larger reversible loss for the 2nd aging which experiences a longer period of storage than others. In addition, the ratio of irreversible/reversible capacity loss at 60 °C is generally lower than that at 25 °C (Fig. A·7), suggesting that the increase in the electronic conductivity with temperature is more predominant than the enhanced side reactions between the cathode and the solid electrolyte at 60 °C. The reversible capacity loss at 60 °C ($\sim$2 mAh g^{-1}) is around two times that at 25 °C ($\sim$1 mAh g^{-1}) for 1 month aging consistent with the increased electronic conductivity at higher temperatures (Figs. A·3 and A·4). Overall, the results provide strong evidence for electronic leakage-induced reversible capacity loss during calendar aging.

To further understand the structural evolution of the cathode composite after long-term storage, we tested the XRD of the cathode after aging at 25 °C and 60 °C (Fig. 6). Despite the slight peak broadening for the cathode aged at 60 °C, no apparent impurities can be observed from the XRD results after aging at 100% SOC for 8 months at 25 °C and 60 °C. While irreversible side reactions between Li_6PS_5Cl and $LiCoO_2$ certainly occurred, the products from these reactions are either amorphous in nature or the content of these phases is too low to be detected from a lab XRD test. Moreover, these irreversible processes did not alter the main structure of $LiCoO_2$ cathodes during long-term aging at quite harsh conditions.

This work highlighted the critical role of reversible self-discharge on the calendar decay of the thiophosphate-based SSBs. The important effect of electronic conduction induced calendar decay is also supported by the voltage decay measurement for solid-state cells with varying electrolyte thicknesses (Fig. A·8), as the cell with a thicker electrolyte has less voltage decay during calendar aging due to the increase in the resistance for electronic leakage. Although irreversible capacity loss due to side reactions between the cathode and the solid electrolyte certainly exists, reversible self-discharge should also be considered for the calendar decay of SSBs. It should be noted that the replacement of a relatively stable $LiNbO_3$-coated $LiCoO_2$ cathode with the start-of-the-art layered oxides such as Ni-rich oxides will lead to more severe side reactions between the cathode and the solid electrolyte, leading to enhanced irreversible capacity loss. However, for practical applications, the thickness of the solid electrolyte should be much lower than 800 μm. Theoretical predictions indicate that the electrolyte thickness needs to be decreased to $<$100 μm or even $<$50 μm to realize the energy density benefit of SSBs, the decrease in the electrolyte thickness will promote the electronic leakage in the SSB.[5,47] Understanding the chemical and structural evolution of the electrodes and their interphases during calendar aging and correlating them with the capacity losses to further understand the decay mechanisms are ongoing in our lab and will be published in our future study. This work calls for more careful evaluations of calendar aging with state-of-the-art cathodes and anodes and with realistic cell form factors. The effect of stack pressure, which has been commonly applied to thiophosphate-based solid-state batteries, on calendar decay should also be carefully studied. The large effect of electronic leakage on calendar aging also requires the development of new methods to qualify calendar decay. The voltage decay method, which measures the decrease of the open circuit potential during storage, may not

fully reflect the real calendar life of the battery under conditions with repeated charging.[18,31] Different aging periods may also need to be used for testing the calendar life of SSBs depending on the charging frequency of the application.

In addition, the study also points to new directions to improve the calendar life of SSBs by lowering the electronic conductivity of solid electrolytes. A rough estimate based on the reversible capacity loss in Figs. 5b and 5c, using Ohm's law, will lead to an electronic conductivity of 3.5×10^{-10} S cm^{-1} at 25 °C and 7.0×10^{-10} S cm^{-1} at 60 °C, consistent with a previous study.[31] The electronic conductivity is several orders of magnitude higher than that of LiPON.[42,48] It should be noted that theoretically, electronic transport in solid electrolytes is driven by Fick's law due to the diffusion of electronic carriers.[49,50] However, the total electronic conductivity including both electron conductivity and hole conductivity under a fixed range of Li activity (or equivalent potentials) can be considered constant because of no change in the defect equilibria of the solid electrolyte, and therefore Ohm's law can be used to roughly estimate the electronic conductivity in the solid electrolyte as well as the electronic leakage induced reversible capacity decay in SSBs. The research advocates a more fundamental investigation of electronic transport in Li solid electrolytes such as voltage dependence, charge carrier, and dominant root causes (grain boundaries, surfaces, impurities, non-stoichiometry etc.) to develop materials solutions to improve the calendar life of SSBs. Many excellent tools, both theoretical and experimental, have already been developed by the solid state ionics community to study electronic transport in oxygen ion conductors for solid oxide fuel cells.[49,51,52] One of the main lessons we learned from the development of Si-containing anodes in liquid-electrolyte LIBs is that, fluoroethylene carbonate (FEC) additive, which was discovered to largely improve the cycling stability, was later found to promote calendar decay.[14,53,54] As many approaches such as doping/substitution used to improve the ionic conductivity or electrochemical stability of solid electrolytes will alter the electronic transport property, more careful evaluation of the electronic conductivity of solid electrolytes should be done during the development of advanced electrolytes for their successful integration in SSBs.

Conclusions

In summary, we analyzed the capacity decay of SSBs with a $LiNbO_3$-coated $LiCoO_2$ cathode, an 800 μm thick Li_6PS_5Cl solid electrolyte, and a Li-In alloy anode during 8-month aging at 100% SOC at both 25 and 60 °C. Over the entire aging test, the capacity of the SSB decreased 4.1% at 25 °C and 7.0% at 60 °C. Notably, capacity loss does not follow a typical power law with aging time, suggesting the complexity of the aging mechanism beyond a typical diffusion-controlled process. Based on a linear extrapolation, the calendar life of the studied SSB is around 1000 days at 25 °C and around 700 days at 60 °C. It is reasonable to expect that the calendar life of SSBs with an advanced cathode such as Ni-rich layered oxides and a thinner electrolyte (<100 μm) will be much shorter, highlighting the critical challenge of calendar decay of thiophosphate-based SSBs. By quantifying the irreversible and reversible capacity losses, we demonstrated a predominant role of reversible self-discharge in the overall calendar decay at both 25 and 60 °C. We also found that the reversible capacity loss increases with the aging time, and the relative contribution of reversible capacity loss increases with temperature, both of which are related to the predominant role of electronic leakage over the irreversible decay processes. The research highlights the importance of reversible capacity loss during calendar aging of thiophosphate-based SSBs and calls for more careful studies on quantifying, understanding, and mitigating calendar aging of SSBs to facilitate their successful utilization in applications where the longevity of batteries is a critical metric.

Experimental

Materials synthesis and characterization.—Li_6PS_5Cl solid electrolyte was prepared by solid-state synthesis method. Li_2S, P_2S_5, and LiCl with a stoichiometric ratio were mixed through ball milling at 110 rpm for 6 h. The mixed powders were vacuum-sealed in a carbon-coated quartz tube and annealed at 550 °C for 24 h. $Li_{0.5}In$ used as the counter and reference electrode was prepared by melting Li and In with an appropriate molar ratio at a temperature of 50 °C higher than the melting temperature. X-ray diffraction measurements were done on a Panalytical X'Pert Diffractometer using a Cu Kα X-ray source.

Cell fabrication.—To prepare a solid-state Li–In/Li_6PS_5Cl/$LiCoO_2$ full cell, 80 mg Li_6PS_5Cl powders were first pressed at a pressure of 100 MPa. A 15 mg cathode composite consisting of $LiNbO_3$ coated $LiCoO_2$ and Li_6PS_5Cl (weight ratio $LiNbO_3$-coated $LiCoO_2$:Li_6PS_5Cl = 70:30) was spread on the top of the solid electrolyte layer. The cathode and solid electrolyte were then pressed together under 350 MPa for 3 min. 100 mg Li–In anode was pressed on the other side of the solid electrolyte under 300 MPa. The initial stack pressure for the cell is 70 MPa. A customized cell consisting of a 10 mm diameter stainless steel die lined with polyether ether ketone (PEEK) and two stainless steel current collector rods was used to test the electrochemical performances of the cells. The stack pressure was controlled using a load cell (FC2331-0000-2000-L). A similar design was also reported from a previous report.[55]

Electrochemical measurements.—The calendar decay of the solid-state cells was tested using Arbin or LAND battery testing systems at 25 or 60 °C. The voltage and current range of the Arbin system is ±5 V (with a 0.02% accuracy) and 100 μA (with a 0.05% accuracy), respectively. The voltage and current range of the LANHE system is 5 V (with a 0.05% accuracy) and 1 mA (with a 0.05% accuracy), respectively. After 5 formation cycles at C/20, the cell underwent a CCCV charging to 4.2 V, followed by seven aging/diagnostic blocks. Each aging/diagnostic block includes an aging period for 1 or 2 months, a discharge process at C/20 directly after aging, two cycles at C/20, followed by a CC charging at C/20 to 4.2 V and a CV charging at 4.2 V for 12 h. A typical constant current (CC) charging and discharging protocol was used for the cells without aging as the control cells. The electronic conductivity of Li_6PS_5Cl solid electrolyte was measured by DC polarization of a two-blocking-electrode using a BioLogic VSP-300 potentiostat. The cell was polarized under a small DC voltage of up to 0.5 V to determine the steady-state current after 12 h. The electrodes for cells were properly insulated and the cells were put in a Faraday cage (BioLogic FC-45) for the electronic conductivity measurement. An ultra-low-current module (BioLogic ULC300) that can lower the base current range from 1 μA to 1 pA was also used with the potentiostat to improve the instrument's resolution to detect small currents. The ionic conductivity of solid electrolytes was measured by electrochemical impedance spectroscopy using a BioLogic VSP-300 potentiostat.

Acknowledgments

The authors acknowledge support from the US National Science Foundation (Award No. DMR-2238672). We thank Drs. Jiyu Cai and Zonghai Chen at Argonne National Laboratory for their help with electrochemical measurements.

Appendix

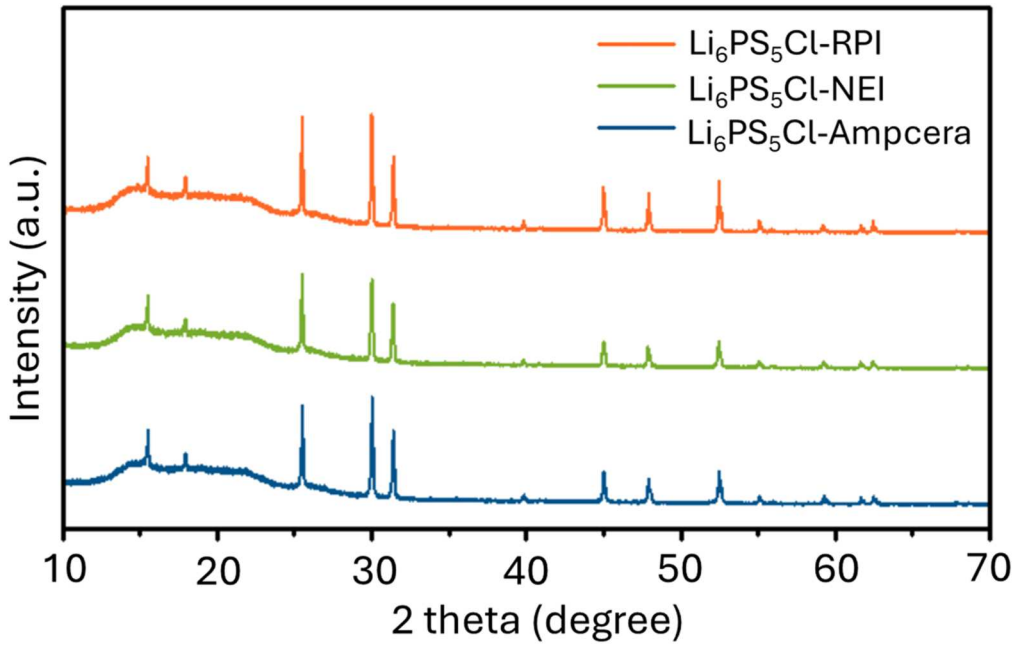

Figure A·1. X-ray diffraction of Li_6PS_5Cl solid electrolytes synthesized in house and from commercial suppliers.

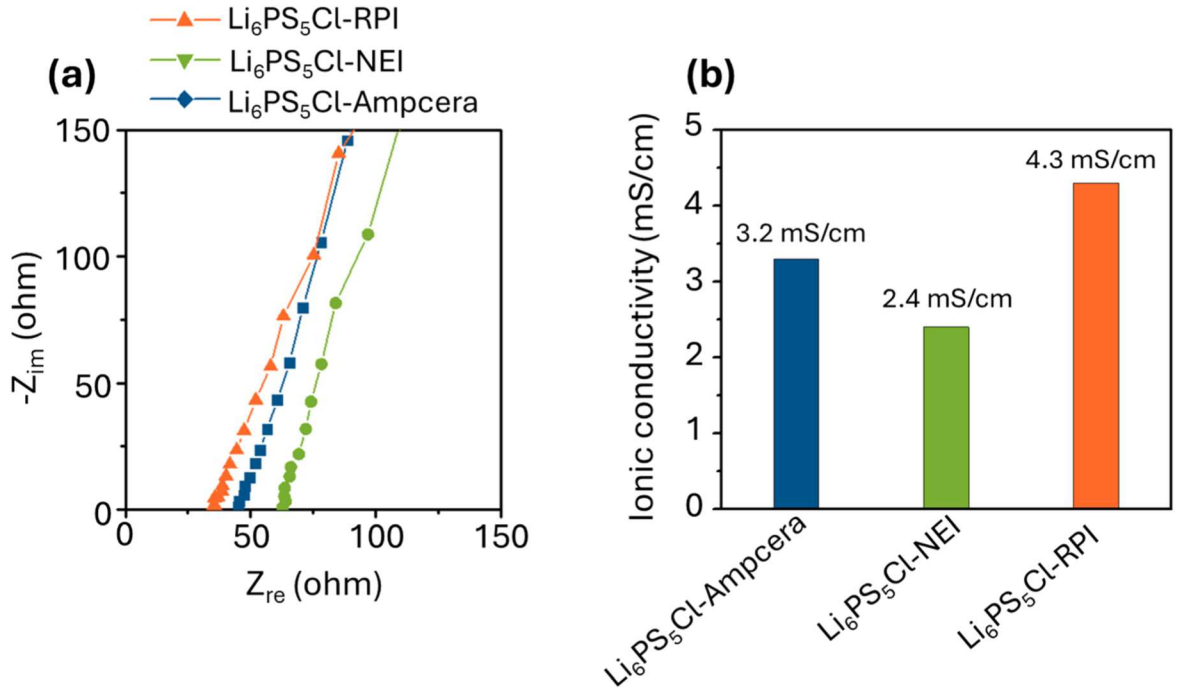

Figure A·2. Impedance spectra (a) and room temperature ionic conductivity (b) of Li_6PS_5Cl solid electrolytes synthesized in house and from commercial suppliers.

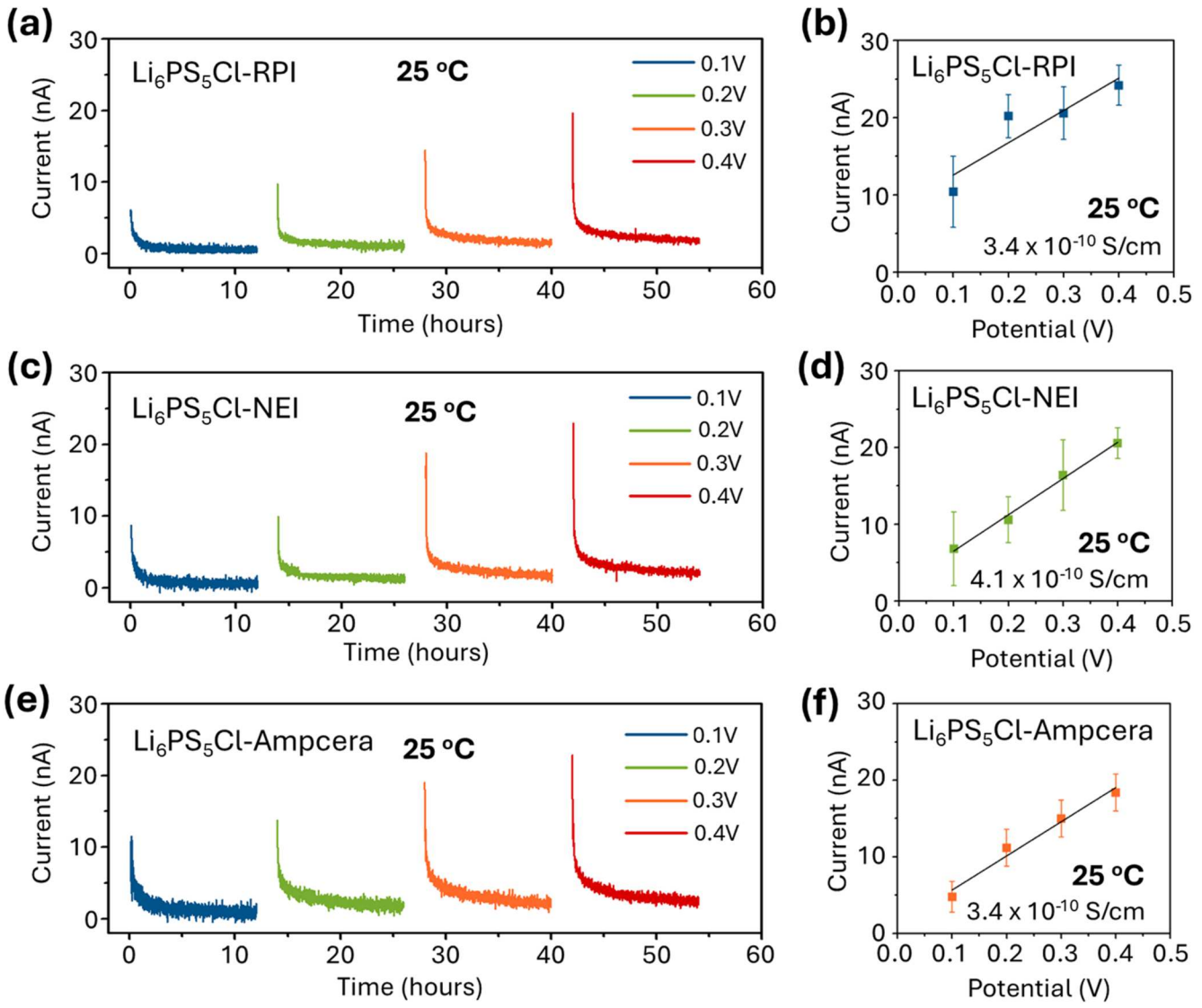

Figure A·3. Current vs time curves during DC polarization (a, c, and e) and electronic conductivities (b), (d), and (f) of Li_6PS_5Cl solid electrolytes synthesized in house and from commercial suppliers at 25 °C.

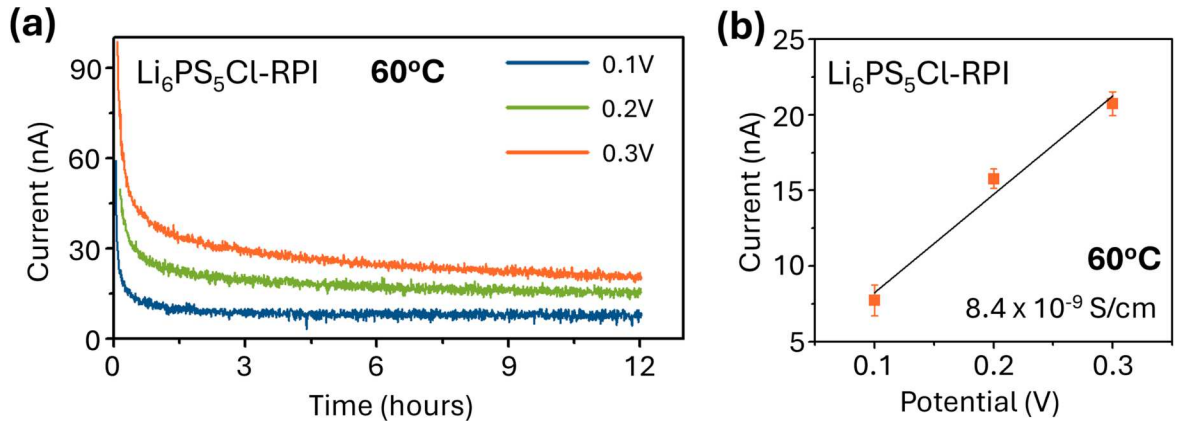

Figure A·4. Current vs time curves during DC polarization (a) and electronic conductivity (b) of Li_6PS_5Cl solid electrolytes synthesized in house at 60 °C.

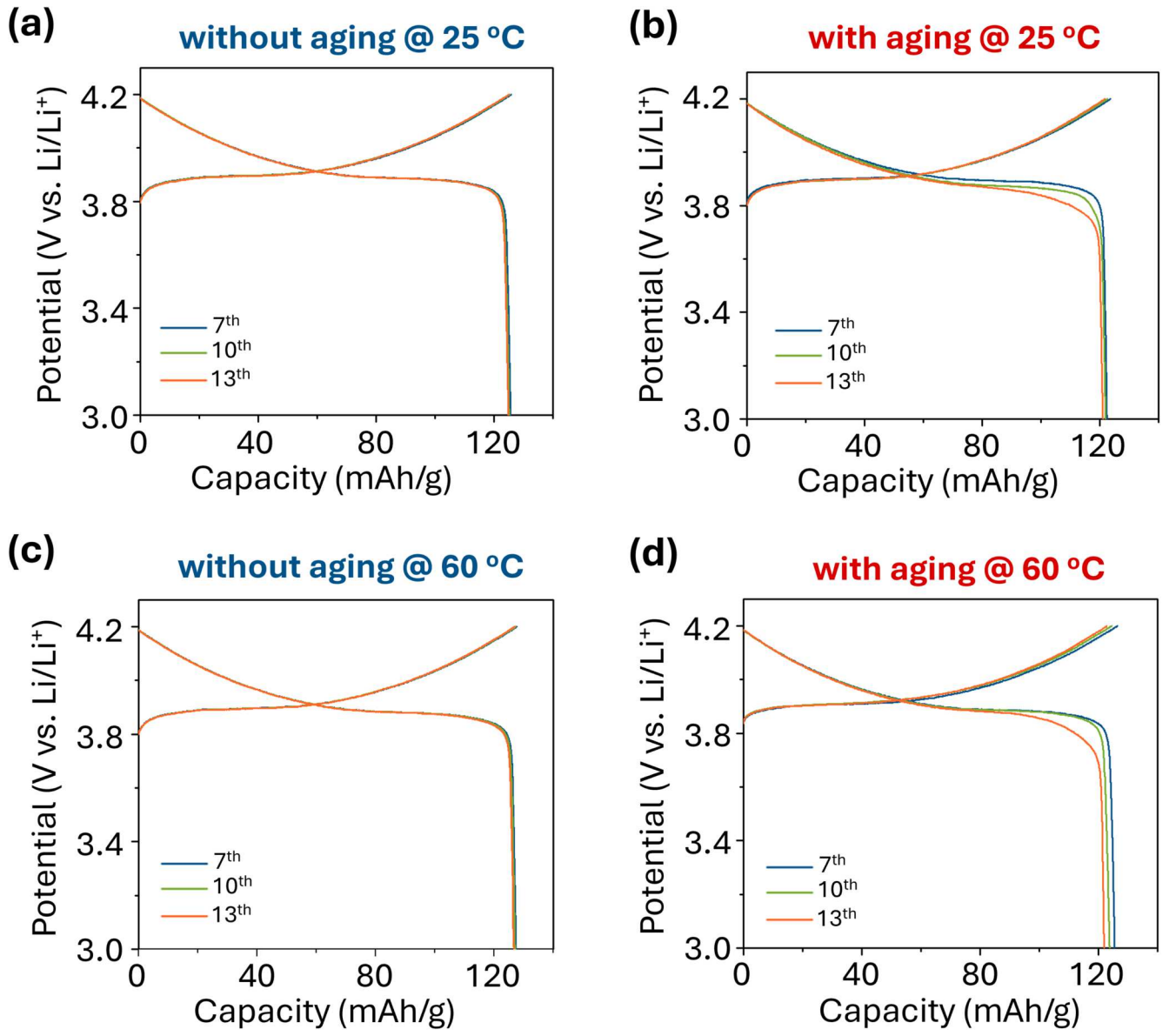

Figure A·5. Charge/discharge curves of solid-state cells with and without aging at 25 and 60 °C.

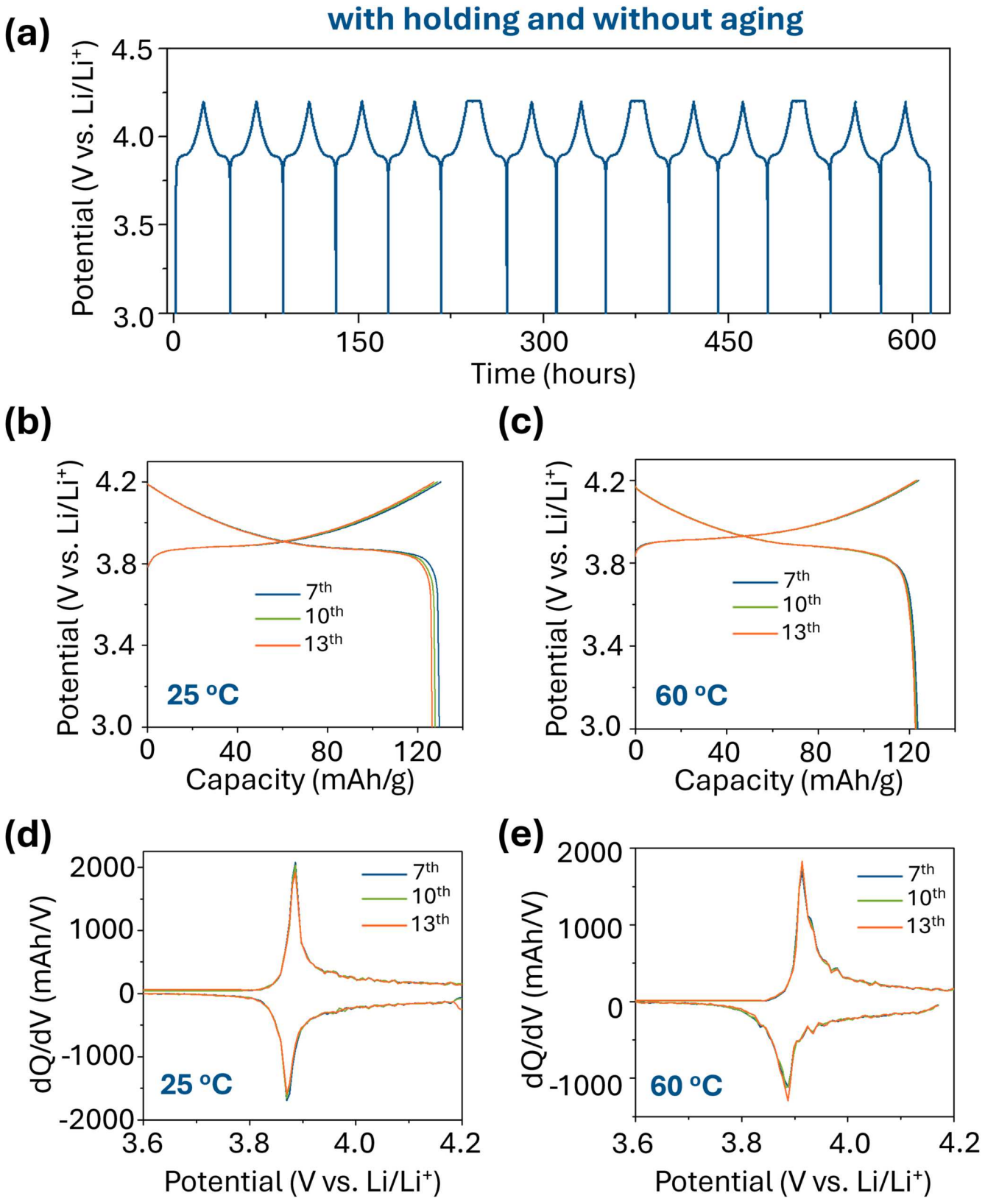

Figure A·6. Voltage vs time curve (a), charge/discharge curves (b and c), and differential capacity vs voltage curves (d and e) of solid-state batteries tested with constant voltage charging but without aging at 25 and 60 °C.

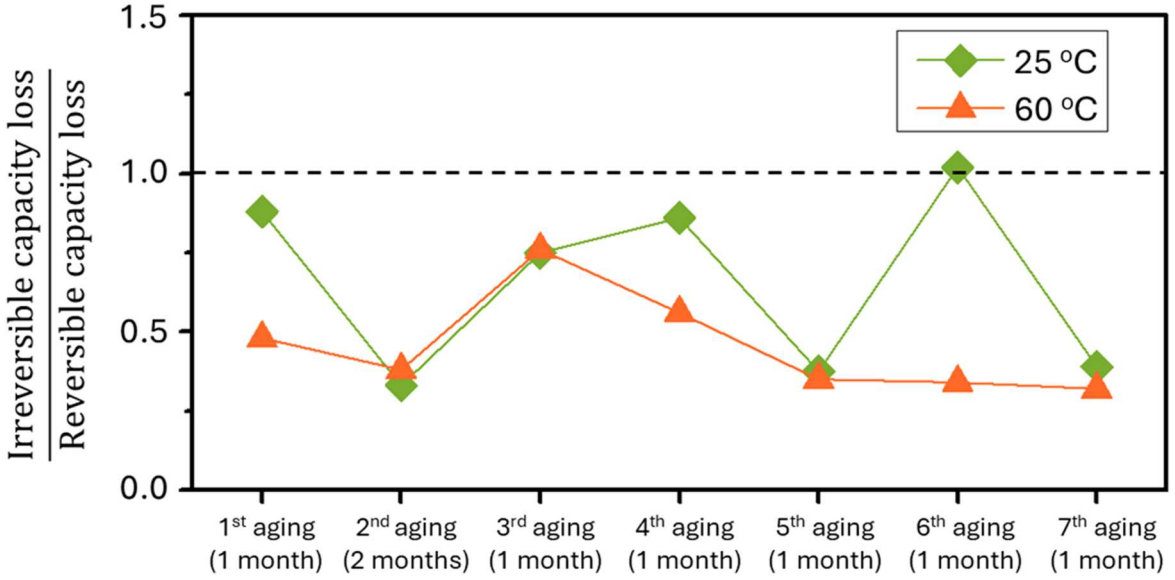

Figure A·7. The ratio of irreversible/reversible capacity loss after each aging at 25 and 60 °C.

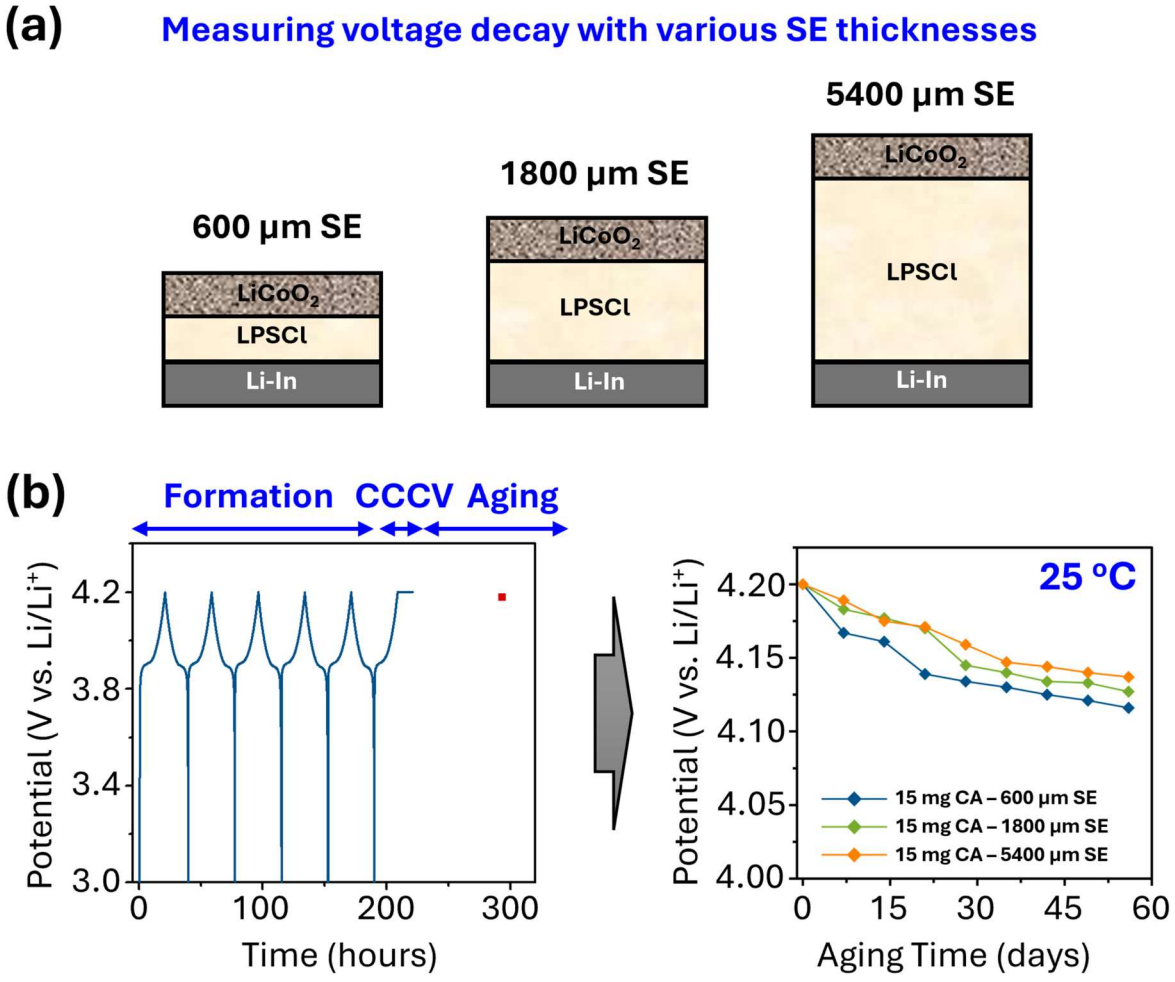

Figure A·8. Measuring voltage decay of solid-state cells with various electrolyte thicknesses during calendar aging. The $LiCoO_2$ cathode loading was fixed at 15 mg for all three cells. Following five formation cycles at C/20, the cells were equilibrated at 4.2 V by a CCCV charging protocol before the aging test.

ORCID

Fudong Han https://orcid.org/0000-0003-2507-4340

References

1. Y. Tian et al., "Promises and challenges of next generation 'Beyond Li-ion' batteries for electric vehicles and grid decarbonization." *Chem. Rev.*, **121**, 1623 (2021).
2. N. Kamaya et al., "A lithium superionic conductor." *Nat. Mater.*, **10**, 682 (2011).
3. Y. Kato, S. Hori, T. Saito, K. Suzuki, M. Hirayama, A. Mitsui, M. Yonemura, H. Iba, and R. Kanno, "High-power all-solid-state batteries using sulfide superionic conductors." *Nat. Energy*, **1**, 16030 (2016).
4. Y. G. Lee et al., "High-energy long-cycling all-solid-state lithium metal batteries enabled by silver-carbon composite anodes." *Nat. Energy*, **5**, 299 (2020).
5. J. Janek and W. G. Zeier, "A solid future for battery development." *Nat. Energy*, **1**, 16141 (2016).
6. S. Randau et al., "Benchmarking the performance of all-solid-state lithium batteries." *Nat. Energy*, **5**, 259 (2020).
7. M. Ecker, N. Nieto, S. Käbitz, J. Schmalstieg, H. Blanke, A. Warnecke, and D. U. Sauer, "Calendar and cycle life study of Li(NiMnCo)O_2-Based 18650 lithium-ion batteries." *J. Power Sources*, **248**, 839 (2014).
8. M. Dubarry, N. Qin, and P. Brooker, "Calendar Aging of commercial Li-Ion cells of different chemistries—a review." *Curr. Opin. Electrochem.*, **9**, 106 (2018).
9. E. Redondo-Iglesias, P. Venet, and S. Pelissier, "Calendar and cycling Ageing combination of batteries in electric vehicles." *Microelectron. Reliab.*, **88–90**, 1212 (2018).
10. P. Keil, S. F. Schuster, J. Wilhelm, J. Travi, A. Hauser, R. C. Karl, and A. Jossen, "Calendar Aging of lithium-ion batteries: I. Impact of the graphite anode on capacity fade." *J. Electrochem. Soc.*, **163**, A1872 (2016).
11. J. Moody, E. Farr, M. Papagelis, and D. R. Keith, "The value of car ownership and use in the United States." *Nat. Sustain.*, **4**, 769 (2021).
12. N. S. Pearre, W. Kempton, R. L. Guensler, and V. V. Elango, "Electric vehicles: How much range is required for a Day's driving?" *Transp. Res. Part C: Emerg. Technol.*, **19**, 1171 (2011).
13. V. N. Lam, X. Cui, F. Stroebl, M. Uppaluri, S. Onori, and W. C. Chueh, "A decade of insights: delving into calendar aging trends and implications." *Joule*, **9**, 101796 (2024).
14. J. D. McBrayer, M.-T. F. Rodrigues, M. C. Schulze, D. P. Abraham, C. A. Apblett, I. Bloom, G. M. Carroll, A. M. Colclasure, C. Fang, and K. L. Harrison, "Calendar aging of silicon containing batteries." *Nat. Energy*, **6**, 866 (2021).
15. M. C. Schulze et al., "Critical evaluation of potentiostatic holds as accelerated predictors of capacity fade during calendar aging." *J. Electrochem. Soc.*, **169**, 050531 (2022).
16. A. Verma, M. C. Schulze, A. M. Colclasure, M.-T. F. Rodrigues, S. E. Trask, K. Pupek, C. Johnson, and D. P. Abraham, "Assessing electrolyte fluorination impact on calendar aging of blended silicon graphite lithium ion cells using potentiostatic holds." *J. Electrochem. Soc.*, **170**, 070516 (2023).
17. J. E. Harlow et al., "A wide range of testing results on an excellent lithium-ion cell chemistry to be used as benchmarks for new battery technologies." *J. Electrochem. Soc.*, **166**, A3031 (2019).
18. L. Streck, T. Roth, P. Keil, B. Strehle, S. Ludmann, and A. Jossen, "A comparison of voltage hold and voltage decay methods for side reactions characterization." *J. Electrochem. Soc.*, **170**, 040520 (2023).
19. M. Kassem, J. Bernard, R. Revel, S. Pélissier, F. Duclaud, and C. Delacourt, "Calendar aging of a Graphite/$LiFePO_4$ cell." *J. Power Sources*, **208**, 296 (2012).
20. I. Zilberman, J. Sturm, and A. Jossen, "Reversible self-discharge and calendar aging of 18650 nickel rich, silicon graphite lithium ion cells." *J. Power Sources*, **425**, 217 (2019).
21. A. J. Smith, J. C. Burns, D. Xiong, and J. R. Dahn, "Interpreting high precision coulometry results on li ion cells." *J. Electrochem. Soc.*, **158**, A1136 (2011).
22. S. E. Sloop, J. B. Kerr, and K. Kinoshita, "The role of li ion battery electrolyte reactivity in performance decline and self-discharge." *J. Power Sources*, **119–121**, 330 (2003).
23. F. D. Han, Y. Zhu, X. He, Y. Mo, and C. Wang, "Electrochemical stability of $Li_{10}GeP_2S_{12}$ and $Li_7La_3Zr_2O_{12}$ solid electrolytes." *Adv. Energy Mater.*, **6**, 1501590 (2016).
24. W. D. Richards, L. J. Miara, Y. Wang, J. C. Kim, and G. Ceder, "Interface stability in solid state batteries." *Chem. Mater.*, **28**, 266 (2016).
25. Y. Xiao, Y. Wang, S. H. Bo, J. C. Kim, L. J. Miara, and G. Ceder, "Understanding interface stability in solid state batteries." *Nat. Rev. Mater.*, **5**, 105 (2020).
26. L. M. Riegger, S. Mittelsdorf, T. Fuchs, R. Rueß, F. H. Richter, and J. Janek, "Evolution of the interphase between argyrodite based solid electrolytes and the lithium metal anode—the kinetics of solid electrolyte interphase growth." *Chem. Mater.*, **35**, 5091 (2023).
27. W. B. Zhang et al., "Interfacial processes and influence of composite cathode microstructure controlling the performance of all-solid-state lithium batteries." *ACS Appl. Mater. Interfaces*, **9**, 17835 (2017).
28. R. Koerver, I. Aygün, T. Leichtweiß, C. Dietrich, W. B. Zhang, J. O. Binder, P. Hartmann, W. G. Zeier, and J. Janek, "Capacity fade in solid state batteries: interphase formation and chemomechanical processes in nickel rich layered oxide cathodes and lithium thiophosphate solid electrolytes." *Chem. Mater.*, **29**, 5574 (2017).
29. A. C. Luntz, J. Voss, and K. Reuter, "Interfacial challenges in solid state Li Ion batteries." *J. Phys. Chem. Lett.*, **6**, 4599 (2015).
30. Y. Huang, B. Shao, and F. Han, "Interfacial challenges in all solid state lithium batteries." *Curr. Opin. Electrochem.*, **33**, 100933 (2022).
31. B. Shao, Y. Huang, and F. Han, "Electronic conductivity of lithium solid electrolytes." *Adv. Energy Mater.*, **13**, 2204098 (2023).
32. B. V. Lotsch and J. Maier, "Relevance of solid electrolytes for lithium-based batteries: a realistic view." *J. Electroceram.*, **38**, 128 (2017).
33. T. Krauskopf, F. H. Richter, W. G. Zeier, and J. Janek, "Physicochemical concepts of the lithium metal anode in solid state batteries." *Chem. Rev.*, **120**, 7745 (2020).
34. S. K. Otto, L. M. Riegger, T. Fuchs, S. Kayser, P. Schweitzer, S. Burkhardt, A. Henss, and J. Janek, "In Situ investigation of lithium metal–solid electrolyte anode interfaces with ToF SIMS." *Adv. Mater. Interfaces*, **9**, 2102387 (2022).
35. S. Wenzel, D. A. Weber, T. Leichtweiss, M. R. Busche, J. Sann, and J. Janek, "Interphase formation and degradation of charge transfer kinetics between a lithium metal anode and highly crystalline $Li_7P_3S_{11}$ solid electrolyte." *Solid State Ionics*, **286**, 24 (2016).
36. S. Wenzel, S. J. Sedlmaier, C. Dietrich, W. G. Zeier, and J. Janek, "Interfacial reactivity and interphase growth of argyrodite solid electrolytes at lithium metal electrodes." *Solid State Ionics*, **318**, 102 (2018).
37. H. Lee, J. Seok, C. Chung, S. Park, J. Kim, and W.-S. Yoon, "Impact of high temperature storage on capacity fading of Ni rich cathodes in sulfide based all solid state batteries." *Chem. Eng. J.*, **498**, 154903 (2024).
38. K. Yoon et al., "Detrimental effect of high temperature storage on sulfide based all solid state batteries." *Appl. Phys. Rev.*, **9**, 031403 (2022).
39. Y. Li et al., "Effects of catholyte aging on high nickel NMC cathodes in sulfide all solid state batteries." *Mater. Horiz.*, **12**, 119 (2025).
40. J. Kang, J. Kim, R. Kim, Y. J. Lim, and J. W. Lee, "Mechanistic insight into calendar aging of anode less all solid state batteries." *Energy Storage Mater.*, **76**, 104164 (2025).
41. Y. Wu, Z. Zhang, D. Wu, F. Xu, M. Zhou, H. Li, L. Chen, and F. Wu, "Calendar aging of sulfide all solid state batteries." *SSRN* (2025).
42. N. J. Dudney, "Solid state thin film rechargeable batteries." *Mater. Sci. Eng. B*, **116**, 245 (2005).
43. N. Ohta, K. Takada, I. Sakaguchi, L. Zhang, R. Ma, K. Fukuda, M. Osada, and T. Sasaki, "$LiNbO_3$ coated $LiCoO_2$ as cathode material for all solid state lithium secondary batteries." *Electrochem. Commun.*, **9**, 1486 (2007).
44. A. Karger, S. E. J. O'Kane, M. Rogge, C. Kirst, J. P. Singer, M. Marinescu, G. J. Offer, and A. Jossen, "Modeling particle versus SEI cracking in lithium ion battery degradation: why calendar and cycle aging cannot simply Be added." *J. Electrochem. Soc.*, **171**, 090512 (2024).
45. T. K. Truong, G. Whang, J. Huang, S. E. Sandoval, and W. G. Zeier, "Probing solid state battery aging: evaluating calendar vs cycle aging protocols via time resolved electrochemical impedance spectroscopy." *J. Mater. Chem. A*, **13**, 17261 (2025).
46. V. Knap, D.-I. Stroe, R. Purkayastha, S. Walus, D. J. Auger, A. Fotouhi, and K. Propp, "Reference performance test methodology for degradation assessment of lithium–sulfur batteries." *J. Electrochem. Soc.*, **165**, A1601 (2018).
47. J. Janek and W. G. Zeier, "Challenges in speeding up solid state battery development." *Nat. Energy*, **8**, 230 (2023).
48. J. Li, N. J. Dudney, J. Nanda, and C. Liang, "Artificial solid electrolyte interphase to address the electrochemical degradation of silicon electrodes." *ACS Appl. Mater. Interfaces*, **6**, 10083 (2014).
49. W. Weppner and R. A. Huggins, "Electrochemical methods for determining kinetic properties of solids." *Annu. Rev. Mater. Sci.*, **8**, 269 (1978).
50. W. Weppner and J. Liu, "Polarization studies of the electronic minority charge carriers in Ag^+ β'' Alumina." *Z. Naturforsch. A*, **46**, 409 (1991).
51. R. A. Huggins, "Simple method to determine electronic and ionic components of the conductivity in mixed conductors: A review." *Ionics*, **8**, 300 (2002).
52. R. A. Huggins, "Use of defect equilibrium diagrams to understand minority species transport in solid electrolytes." *Solid State Ionics*, **143**, 3 (2001).
53. T. Hou, G. Yang, N. N. Rajput, J. Self, S. W. Park, J. Nanda, and K. A. Persson, "The influence of FEC on the solvation structure and reduction reaction of $LiPF_6$/EC electrolytes and its implication for solid electrolyte interphase formation." *Nano Energy*, **64**, 103881 (2019).
54. R. Jung, M. Metzger, D. Haering, S. Solchenbach, C. Marino, N. Tsiouvaras, C. Stinner, and H. A. Gasteiger, "Consumption of fluoroethylene carbonate (FEC) on Si C composite electrodes for Li ion batteries." *J. Electrochem. Soc.*, **163**, A1705 (2016).
55. T. A. Yersak, J. R. Salvador, N. P. W. Pieczonka, and M. Cai, "Dense, melt cast sulfide glass electrolyte separators for Li metal batteries." *J. Electrochem. Soc.*, **166**, A1535 (2019).